DOI: 10.2478/v10077-009-0013-1

K. Szybowska[1], M. Gazda[2], A. Lisowska-Oleksiak[1]
[1] Gdansk University of Technology, Chemical Faculty, Department of Chemical Technology, Gdansk, Poland
[2] Gdansk University of Technology, Faculty of Applied Physics and Mathematics, Department of Solid State Physics, Gdansk, Poland

CHEMICAL CHARACTERISTICS OF NEW NANOPOWDER OF TITANIA DOPED WITH NITROGEN ATOMS

ABSTRACT

Characteristics of new nitrogen doped TiO_2 prepared in an one-pot synthesis where titania (IV) complexes with ligands containing nitrogen atoms were used as a precursor are presented in this paper. The pale yellow nanopowder with crystallite size of 9 – 12 nm is obtained as a product of calcination at 310˚C and repeated washing procedure. Elemental analysis shows that nitrogen (1.087 at. pct.) is present in obtained material. The morphology and microstructure of samples were examined by XRD, AFM, UV-VIS and FTIR-ATR techniques. These studies confirm that obtained powder demonstrates a significant decrease in the band gap energy value (E_g = 2.83 eV) comparing to pure TiO_2 (E_g 3.22 eV). Presence of N-Ti-O bonds was confirmed *via* FTIR ATR. Products of the powder thermal decomposition were detected using TG-DSC technique coupled with mass spectrometry (MS). The report presents electrochemical studies which allow estimation of a flatband potential E_{fb} on the basis of the Mott-Schottky relation.

Key words: *TiO_2, nanomaterials, nitrogen doping, flatband potential, Mott-Schottky plot*

INTRODUCTION

The development of non-polluting and renewable fuels supported by the conversion of solar to electric energy as well as photocatalytic method of air purification is receiving much more attention in present times. In the midst of various important reactions, the water splitting into oxygen and hydrogen by sun radiation is potentially one of the promising ways where the TiO_2 electrodes are used [1]. That is why most investigations have focused on TiO_2 with photocatalytic activity difference to visible light. For the past few decades several attempts have been employed to modify the titanium oxide for use in wavelengths above 300 nm. The most often applied approach is based on doping of transition metals such as Fe [2], Pt [3] into TiO_2 [4, 5], or reduced form of TiO_x. Other popular method relays on the substitute doping of C [6], F [7] S [8, 9] and N [10] instead O atoms in the anatase crystal structure. The easiest and most feasible TiO_2 modification for achieving visible light activity seems to be nitrogen doping [11]. That is why in recent years there is a

continually increasing interest in synthesis of N-doped TiO_2 and its characterization by different methods. Since 2001, when Asahi *et al*. [12] reported the method according to what N-doped titania could be obtained, there have been a lot of reports considering different synthesis. Some of them consider sputtering of TiO_2 in an N_2-Ar atmosphere, the hydrolysis of organic or inorganic titanium precursors such as titanium tetraisopropoxide [13, 14], titanium (IV) sulphate [15] with ammonia aqueous electrolyte following heating of the resultant precipitates, and the calcining of TiO_2 powder with urea [16]. Getting particle size as smallest as possible appeared to be of great importance. One of the latest methods concerning using soluble salt matrix takes advantage of NaCl giving crystalline TiO_2 particles about 15 nm in diameter [17]. This idea was taken into account on planning the presented synthesis of N-doped TiO_2 nanopowder. Another advantage of a large amount of salt co-precipitated with the oxide is the specific surface area and low pore volume. This influence on undoped TiO_2 was recently presented by Bianchi *et al*. [18]

Apart from photocatalytic properties of titanium dioxide, this material has also semiconducting and electrochemical properties and due to them, the anodic formation of compact layers of TiO_2 in different electrolytes is extensively investigated [19]. The study of metal/semiconductor and semiconductor/electrolyte Schottky barriers is very important in view of many applications of these systems in photodetection and solar energy conversion [20, 21]. That is why studies are carried out implying determination of certain fundamental parameters of the barrier, such as the effective donor and acceptor density [22], the flat-band potential [23], the position of the conduction and valence band edges [24]. These experiments and calculations concern TiO_2 electrode material in aqueous as well as in nonaqueous media [25]. What is more, it is very hard to find ranked data about N-doped titanium even though the way to obtain powder with incorporated nitrogen atoms, preparation manner of electrodes, type of electrolyte make a significant effect on the electrochemical activity of TiO_2.

In this paper, nitrogen doped TiO_2 was prepared *via* an one-pot method where titanium (IV) complexes with ligand containing nitrogen atom were used as a titania precursor. The particles of TiO_2 arising during synthesis were surrounded by nitrogen source and NaCl. After repeated washing and rinsing procedure followed by calcination at 310˚C yellow powder was received. This technology is very simple and allows obtaining nanosized particles. The morphology and microstructure of samples were examined by UV – VIS, XRD, AFM and FTIR ATR. The report presents impedance spectroscopy measurements which allow determining flatband potential of nitrogen doped electrode material.

EXPERIMENTAL PROCEDURES

Synthesis and course of electrochemical experiment

The modified TiO_2 powder was obtained by the method subscribed in Polish patent application [26]. The main idea of this method relies on the use of the Ti (IV) compound containing Ti-N bond as a precursor for TiO_2 formation. Without disclosing patent claims, according to this description an amount of 4.5 – 5.5 M MeOH (Me – alkali metal) and 10 -

MOST WIEDZY Downloaded from mostwiedzy.pl

30% H_2O_2 was added to Ti (IV) complex solution in aprotic solvent. The mixture was vigorously stirred in an ice water bath. After 21 hours the liquid phase was evaporated and then the precipitate was calcined at 310˚C in a quartz reactor for different periods of time. The obtained material was washed with a solution of ethanol/ water (80:20) to eliminate the salt and centrifugally separated for 10 minutes at 12500 RPM speed (High Speed Brushlers Centrifuge MPW - 350R). This procedure was repeated several times and finally the precipitate was dried at 100˚C. To study this material in electrochemical way slurry was deposited as a layer on titanium (Aldrich titanium foil, 0.127 nm thick, 99.7%) plate – shaped electrode. Prior to deposition, the titanium substrates were rinsed in ethanol for 5 s and air dried. The Ti substrate electrodes were then carefully cleaned in a HCl : H_2O (7:1 volumetric ratio) solution for 10 s, and rinsed with distilled water [27]. Subsequently an amount of suspension was spotted on clean substrates and then calcined at 310˚C for 1 h in a furnace with quartz tube opened to air. After getting the ambient temperature prepared electrodes with N–doped TiO_2 layer (0.5 cm^2) were washed with distilled water and then they were ready to be use in electrochemical and AFM experiments.

Instruments

The electrochemical experiments were performed using the potentionstat – galvanostat system AutoLab PGStat 10 in a standard three–electrode assembly, wherein the Ti foil covered by the N-doped TiO_2 layer was used as working electrode, a Pt mesh as a counter electrode and an Ag/AgCl (0.1 M KCl) as a reference electrode. All potentials given in this work were recalculated versus a SCE. Cyclicvoltammetry and electrochemical impedance spectroscopy measurements were carried out. Three electrodes were immersed in one compartment cell containing 0.5 M Na_2SO_4 (pH = 7.7). Experiments for two various types of electrodes were repeated twice and their reproducibility was found to be satisfactory in respect to qualitative representation of electrode/electrolyte interface.
The UV - VIS reflectance spectra of the powders were measured on UV – Vis spectrophotometer (Perkin Elmer Lambda 10) which was equipped with diffuse reflectance accessory (Labsphere, North Sutton). All obtained reflectance data were recalculated using the Kubelka-Munk function providing determination of the new material's energy bandgap.
The infrared analyses were carried out on the calcined powder by using a Thermo Nexus 870 FTIR spectrometer accomplished with an attenuated total reflectance (ATR) accessory (Labsphere).
The Atomic Force Microscopy (AFM) was used to take a high resolution picture of the surface of obtained powder deposited as a layer on the titanium substrate. The image was made on Solver-Next microscope.
The phase structure of the N – doped TiO_2 powder calcined at 310˚C for different periods of time was identified by powder X – ray diffraction method (XRD). The samples were examined by Philips X'Pert diffractometer employing Cu-Kα radiation (λ = 1.54178 Å). The XRD patterns were recorded with 2θ in range 20 – 65 by step scanning, using a fixed counting time of 2 s/step and 2θ increments of 0.02. Average crystallite size was calculated from full width at half-maximum according to Scherrer's equation:

$$D = \frac{0.89\lambda}{B\cos\theta} \tag{1}$$

MOST WIEDZY Downloaded from mostwiedzy.pl

where λ is the wavelength of X–ray radiation, *B* is the full width of half-maximum height of the most intense peak and *D* standing for crystalline size. The line broadening due to the instrument (main source of error) was calculated from Warren–Averbach's method and was eliminated from the crystallite size determination.
In order to determine the phase contribution in the synthesized powder calculations considering the intensity of the strongest anatase (101) and rutile (110) peaks reflection were carried out according to the equations [28]:

$$W_A\% = \frac{100\%}{1+1.265\frac{I_R}{I_A}} \tag{2}$$

$$W_R\% = 100 - W_A\% \tag{3}$$

where W_A% and W_R% appropriately is anatase and rutile percentage by weight, I_A and I_R is respectively anatase and rutile intensity of the highest peak.
The doped sample was analyzed by thermogravimetric (TG) and differential scanning calorimetry (DSC) in $\alpha - Al_2O_3$ pan with a NETZSCH STA449F3 coupled with mass spectroscopy (MS). This thermal analysis system worked under argon gas flow 0.02 dm^3/min. from 293 to 1273 K at a heating rate of 10 $Kmin^{-1}$.

RESULTS AND DISCUSSION

XRD spectrometry

X–ray diffraction patterns of prepared samples before and after washing procedure are presented in Figure 1 (a and b). As it can be seen, there are peaks which are typical for anatase and rutile, crystal phases of TiO_2 [29]. Using the Scherer's equation (1) the crystallite size could be obtained and on the basis of equations (2) and (3) crystallite phase contribution could be estimated. Obtained results were collected in Table 1. For all of the examined samples the content of rutile and anatase is similar and an average crystallite size is within 9 and 12 nm. These nano–size particles were obtained thanks to the titania co-calcination with simple water soluble salt. Inert salt (Figure 1 b) can prevent the growth of rising particles during synthesis and control their distribution [30, 31]. After the repeated rinsing procedure salt was washed out and separated nanoparticles of titania were obtained [32 – 34].

MOST WIEDZY Downloaded from mostwiedzy.pl

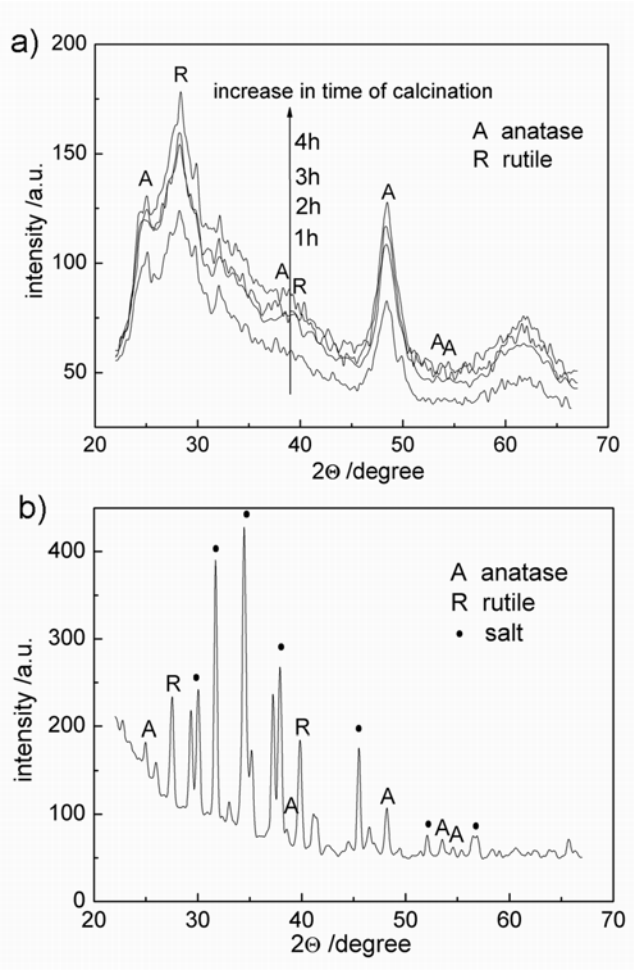

Fig. 1. Powder X-ray diffraction paterns for (a) cleaned powder calcined for different periods of time (1 – 4 h) at 310ºC and (b) unwashed sample

Table 1. *The calculated crystallite size and phase contribution for calcined samples*

Sample	Phase contribution Anatase/Rutile	Crystallite size /nm
1h	41.4/58.6	12.8
2h	41.7/58.3	10
3h	43.6/56.4	9.2
4h	40.6/59.4	9

Atomic Force Microscopy

The dimension of particles and their distribution were confirmed also by AFM image. In Figure 2 a picture of the obtained powder as a layer on the titanium substrate is shown. That layer, about 10 μm in thickness, was made by drop-coating. Because of the use of the imprecise coating method only in some areas nice well shaped, small grains could be observed. Taking into consideration the scale it could be said that they are in

MOST WIEDZY Downloaded from mostwiedzy.pl

a nanodimension scale. Thus, both methods atomic force microscopy and X–ray diffraction powder spectrometry confirm each other in respect to the size of titania particles.

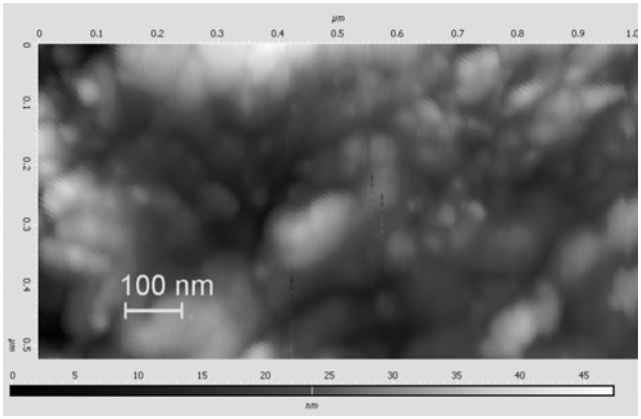

Fig. 2. AFM image of the surface of N-doped TiO_2 deposited on the titanium foil

Diffuse Reflectance Spectroscopy

The optical reflectance spectroscopy was used to study the capability to photosensitization by obtained nanoparticles. The shift in value of the bandgap energy for modified powder in comparison to undoped TiO_2 can be observed from the Kubelka-Munk plots presented in Figure 3. Such change is known to occur where nitrogen atoms are incorporated into the structure [13]. The bandgap energy (a) for pure TiO_2 (Aldrich) nanopowder equals 3.22 eV (as known from literature) and for doped material it equals (b) 2.83 eV. Thus the energy gain is estimated as 0.39 eV. In comparison to Kisch. *Et al*. [35] one may consider the obtained result as satisfactory. The colour of samples calcined for 1 or 2 h was pale yellow whereas longer time of calcination brought about that powders became slightly darker. Some authors, i.e. Y. Zhao *et al.* consider this effect as a result of the organic residues carbonization because of high calcining temperature [36].

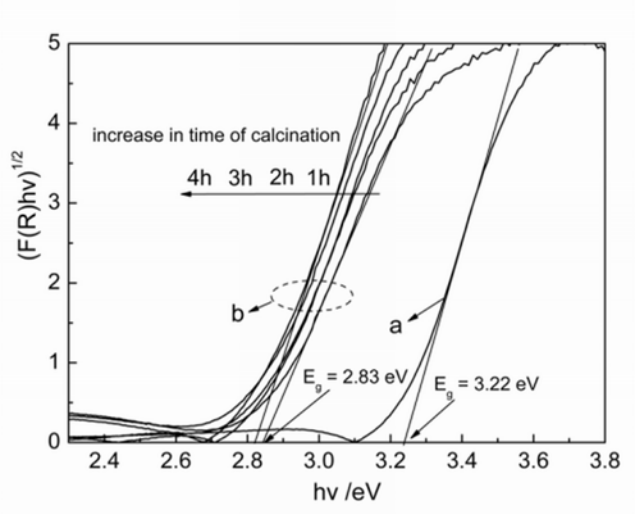

Fig. 3. The Kubelka-Munk plot for (a) TiO_2 (Aldrich) and (b) modified powder samples obtained after different time of calcinations (1 – 4h) at 310ºC

MOST WIEDZY Downloaded from mostwiedzy.pl

Elemental analysis was done for the sample calcined for 4 h. The atomic percent of nitrogen was 1.087 % what gives strong evidence of doping phenomenon. On the basis of this data the empirical formula of obtained powder was estimated as $TiO_{1.938}N_{0.062}$.

FT–IR ATR

Figure 4. compares the infrared absorption spectra for the TiO_2 (Aldrich) and for prepared N–TiO_2 powders. FT–IR ATR spectra provide information about surface functional groups. The samples calcined for different periods of time exhibit similar FT-IR spectra. The modified nano-powders showed the main, broad band in the range 400 – 700 cm^{-1}, which was attributed to Ti–O stretching and Ti–O–Ti bridging stretching modes [11]. The new sensitized material varies in comparison to undoped TiO_2 as four new peaks: 910 cm^{-1}, 1060 cm^{-1}, 1640 cm^{-1} and 3350 cm^{-1} appear and no NH_4^+ absorption peak is observed. First of them is attributed to peroxides adsorbed at TiO_2 surface such as Ti–OOH. Another new absorption peak at 1060 cm^{-1} indicates that some nitrogen atoms have replaced the oxygen atoms of TiO_2 lattice to form pale yellow nitrogen-doped TiO_2. It can be assigned to the N-Ti–O stretching vibrations [37 - 39]. The new strong peak at 1640 cm^{-1} was attributed to bending vibrations of O–H and N–H, and broad one at 3350 cm^{-1} was stretching vibrations O-H and N-H [11]. The IR spectra of the as-prepared powder revealed that Ti–O, N–H, TiO–H, Ti–OOH and N–Ti–O groups existed on the surface of the sample prepared by hydrothermal process. The observing N–Ti–O vibrations could indicate that nitrogen atoms were incorporated into the lattice of TiO_2 as well.

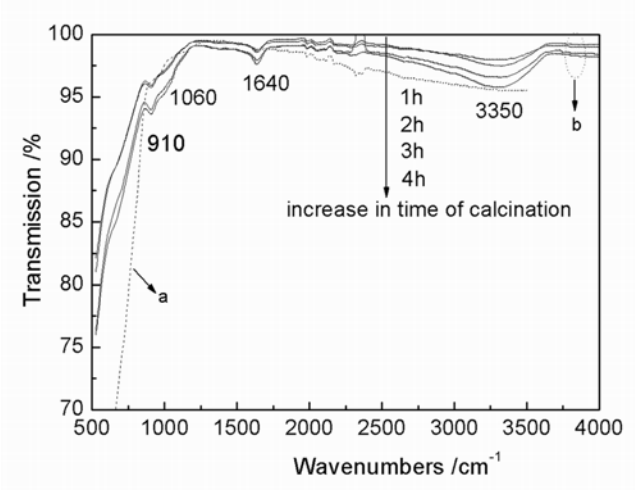

Fig. 4. FT-IR ATR spectra of (a) TiO_2 (Aldrich) and (b) modified powder samples obtained after different time of calcinations (1 – 4h) at 310ºC

Thermal Analysis coupled with MS

To understand the stability of as-prepared powders the thermal behaviour of 4 h sintered sample was investigated. The weight loss curve is showing that in the range from ambient temperature up to 500ºC the sample lost 4.7 % of its initial weight. This loss is found to be

MOST WIEDZY Downloaded from mostwiedzy.pl

lower than observed by other researches, even above 20 % [13]. The riddance of mass could be attributed to desorption of water and carbon dioxide out of the surface [40]. Given explanation is proven by the shape of DSC curve in the Figure 5. a).

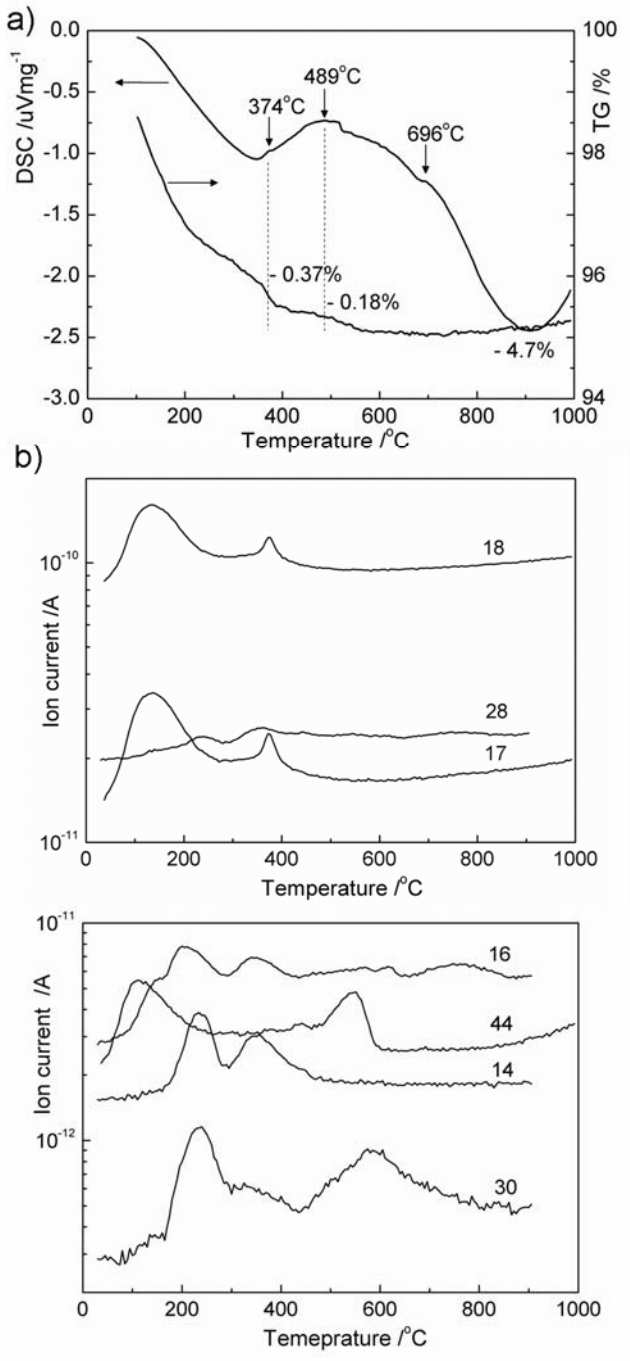

Fig. 5. a) TG-DSC curves for sample calcined through 4 h at 310ºC.
b) Ion current of selected mass-to-charge number attributed to appropriate ions (see Table 2)

MOST WIEDZY Downloaded from mostwiedzy.pl

The endothermic broad band is recorded in the same extend where the decline in mass is the highest, see Figure 5a. Another three peaks on the DSC curve are located at 374ºC, 489ºC and 696ºC. They all have exothermic character, and the first of them is connected with noticeable change in mass (- 0.37 %), while for the second one the decrease in mass is quite slight (- 0.18 %). The peak at 696ºC do not show any weight loss which should be attributed to the phase transformation from anatase to rutile [28]. Changes of ion currents for selected ions with temperature are shown in Figure 5 b). Data presented in the Table 2 reveals formulas assigned to selected mass-to-charge ratio including oxygen, nitrogen, hydrogen and carbon, for which the detector was set [41].

Table 2. *Selected mass-to-charge ratio with the attributed formulas.*

M/Z	Formula
14	N
16	O
17	OH, NH_3
18	H_2O
28	N_2, CO
30	NO
44	N_2O, CO_2

The comparison of ion currents courses (from MS) with TG-DSC curves gave information about species which left the sample in the specific temperature range. In the range up to 200ºC the sample looses mainly adsorbed water, hydroxyl groups and carbon dioxide. The ion peaks about 200ºC which are assigned to 14, 16, 30 mass-to-charge ratio, suggested that there exists decline of nitrogen, oxygen and nitrogen monooxide ions. The relation between exothermic peak located at 374ºC and ion currents of 14, 16, 17, 18, 28, 30 mass-to-charge ratio shows that in the lattice and/or on the surface there appears some bonds' breaks. The main DSC-peak at 489ºC could be connected with the increasing ion current of 30 and 44 ion-to-charge ratio. It clearly indicates that there exists rupture which leads to release NO and N_2O species. Because this process takes place in such a high temperature it could be said that the bond breaks inside the lattice. The given description about changes in ion currents and their relation with DSC curve one may interpret as a confirmation that nitrogen atoms exist on the surface and in the lattice as well.

Electrochemical impedance measurements

Impedance spectroscopy measurements of new material were performed to obtain data allowing the characterization of interfacial properties of the boundary between the deposited N – doped TiO_2 layer and aqueous electrolyte [42]. The procedure requires the collection of impedance spectra in the chosen frequency range taken for the material used as a working electrode. The working electrode undergoes DC stepwise polarization starting from the rest potential. As a rule, impedance spectroscopy requires steady state conditions during entire collection of the data, otherwise they are not credible and measurements should avoid nonlinearity between applied potential and current response. That is why the experiment was carried out in the potential range where faradic processes, *i.e*. adsorption with charge transfer were under control and were taken into consideration during application of an electric equivalence circuit (EQVC). Cyclic voltammetry tests were

MOST WIEDZY Downloaded from mostwiedzy.pl

applied to establish non-faradic potential range of electrode polarization (Figure 6.). Observed curves both for native titania on the titanium foil and studied powder covering titanium substrate did not show any significant increase in current in the studied potential range.

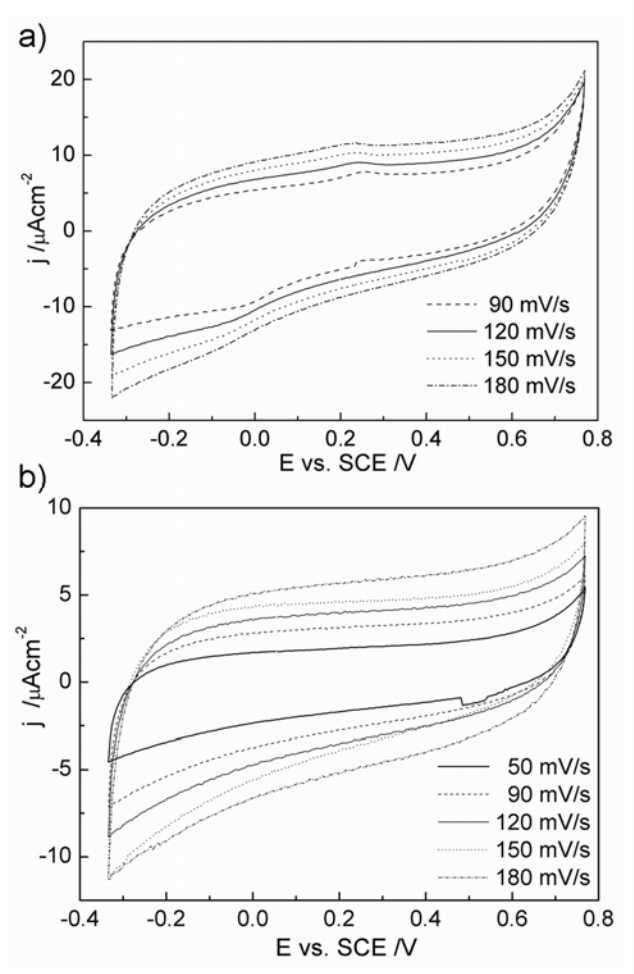

Fig. 6. Cyclic voltammetry curves obtained for (a) titanium foil with a passive layer and (b) N-doped TiO_2 deposited on the titanium foil as a working electrodes immersed in 0.5 M Na_2SO_4 with different sweep rates

Complex plane impedance plots for the titanium foil with native passive layer and N-doped TiO_2 on the titanium foil are presented in Fig.7. The whole frequency range spreads from $f = 20$ kHz to 0.1 Hz with 10 points per decade and 10 mV amplitude of AC signal. The main feature of impedance spectra is almost a vertical line, typical for a capacitive element. However, accurate analysis of obtained data requires application of more detailed electrical equivalent circuit. In this case the EQVC constructed of resistive and capacitive elements connected as it is shown in the Figure 7 was proposed.

MOST WIEDZY Downloaded from mostwiedzy.pl

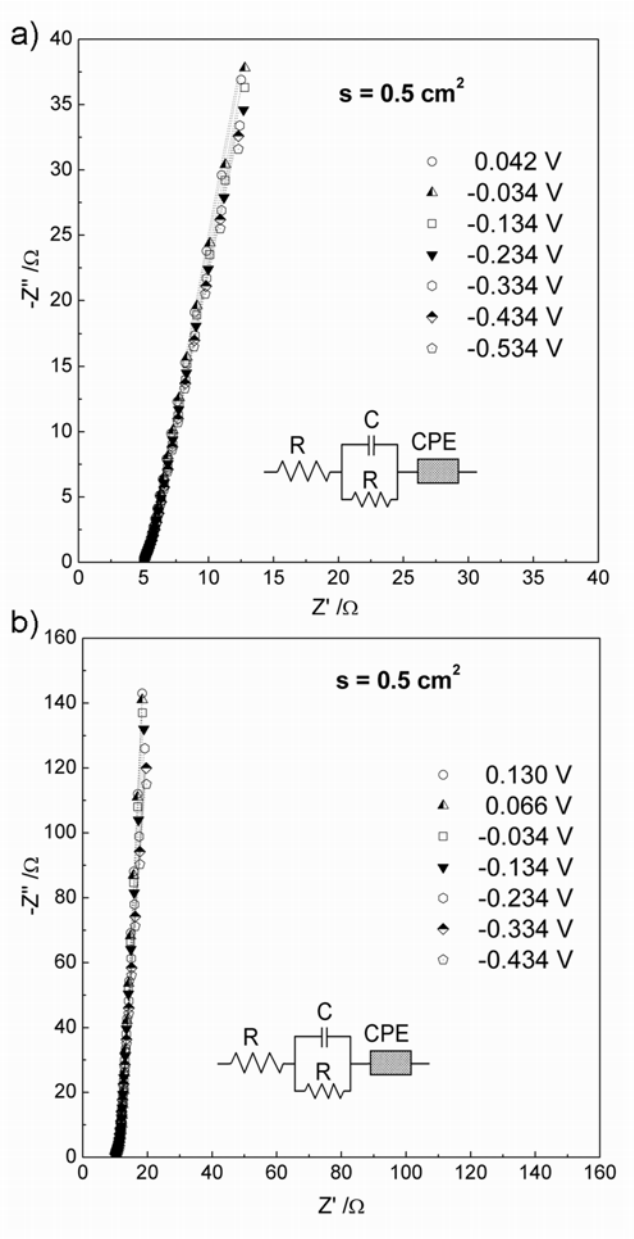

Fig. 7. Complex plane impedance plots for (a) titanium foil with a passive layer and (b) N-doped TiO_2 on the titanium foil in 0.5 M Na_2SO_4 for different potentials (f = 0.1 Hz ÷ 20 kHz) and its fitting line calculated on the basis of the electrical equivalent circuit

There are ***R_e(RC)CPE***, where
R_e – electrolyte resistance
RC – interpreted as resistance and capacitance of adsorbed species or according to Gordon and Gomes [24] should reflect presence of outer Helmholtz layer
CPE – constant phase element, attributed to capacitance of space charge region (C_{sc})
Impedance of *CPE* is given by:

$$Z_{CPE} = (\omega)^{-n} Q^{-1} \tag{3}$$

MOST WIEDZY Downloaded from mostwiedzy.pl

n ($0 < n < 1$), Q – characteristic constants for *CPE* and $\omega = 2\pi f$ – angular frequency. The value n is related tothe rotation angle α of the spectra:

$$\alpha = (1 - n) \cdot 90° \tag{4}$$

The fitting procedure was performed using EQIVCRT program [43] with good accuracy ($\chi^2 = 10^{-6} \div 10^{-5}$). In the studied case n varied from 0.86 to 0.95. Assuming that calculated Q values represent C_{sc} the Mott-Schottky plots of pure titanium foil and N-doped TiO_2 on titanium foil were prepared (Figure 8.). As it can be seen a determination coefficient is very high. Owing to the application of the whole fitting procedure established capacitance is interpreted as capacitance of the space-charge region [44].

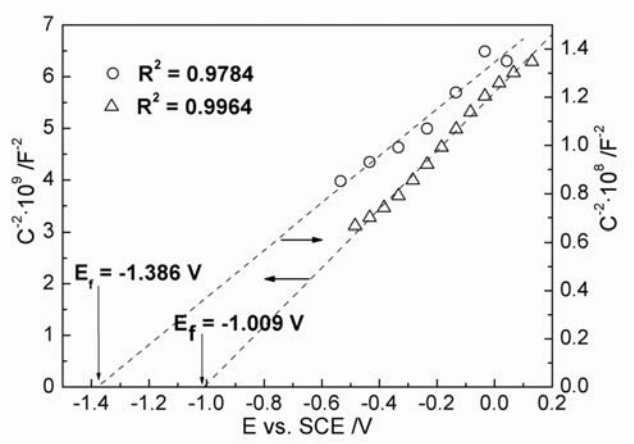

Fig. 8. The Mott-Schottky plot of (○) titanium foil with a passive layer and (△) N-doped TiO_2 on the titanium foil measured at various potentials

The intercept of the Mott-Schottky plot gives the value of flatband potential E_f. The flat band potential of the new material is shifted by 0.377 V towards anodic range what is desirable for an ideal semiconductor photocatalyst. Similar direction of E_f shift but much smaller (only 40 mV) was observed by Colussi *et al.* [45]. However, these researchers found that nitrogen doped titanium fails to catalyze the oxidation of organic impurities under visible illumination. On the other hand further studies in this direction are necessary and planned.

CONCLUSIONS

Nitrogen doped TiO_2 nanopowder was synthesized from Ti (IV) complexes with ligands containing nitrogen atoms. Tailoring of nanosize diameter of titania particles was possible by co-precipitation and calcination in the presence of the water soluble salt. The elemental analysis, FT–IR ATR spectra, TG–DSC analysis coupled with the MS confirmed presence of nitrogen atoms in the selected samples. The nitrogen doping phenomena resulted in the

MOST WIEDZY Downloaded from mostwiedzy.pl

shift of absorbance maxima towards visible wavelength was achieved as expected. The flatband potential of N–doped TiO_2 determined (in 0.5 M Na_2SO_4) on the basis on fitting procedure using EQVC was shifted by 0.377 V in comparison to native TiO_2 on the titanium foil. Further studies concerning electrochemical and photocatalytic characterization of doped TiO_2 are necessary.

ACKNOWLEDGMENTS

This work was supported by the BW014694/T.042, Gdansk University of Technology.
The authors wish to thank dr E. Hebanowska from University of Gdansk for her helpful contribution into completing the research tests on TG DSC analysis.

REFERENCES

1. Fujishima A., Honda K.: Electrochemical Photolysis of Water at a Semiconductor Electrode. Nature 238 (1974) 37-38.
2. Damm C.: An acrylate polymerization initiated by iron doped titanium dioxide. Journal of Photochemistry and Photobiology A: Chemistry 18 (2006) 297-305.
3. He C., Xiong Y., Shu D., Zhu X., Li X.: Preparation and photoelectrocatalytic activity of Pt(TiO_2)-TiO_2 hybrid films. Thin Solid Films 503 (2006) 1-7.
4. Ghosh A. K., Maruska H. P.: Photoelectrolysis of Water in Sunlight with Sensitized Semiconductor Electrodes. Journal of Electrochemical Society 124 (1977) 1516-1522.
5. Anpo M.: Photocatalysis on titanium oxide catalysts: Approaches in achieving highly efficient reactions and realizing the use of visible light. Catalysis Surveys from Japan 1 (1997) 169-179.
6. Irie H., Watanabe Y., Hashimoto K.: Carbon-doped TiO_2 powders as a visible-light sensitive photocatalyst. Chemistry Letters 32 (2003) 772-773.
7. Yu J. C., Yu J. G., Jiang Z., Zhang W. K.: Effects of F^- Doping on the Photocatalytic Activity and Microstructures of Nanocrystalline TiO_2 Powders. Chemistry of Materials 14 (2002) 3808-3816.
8. Ho W., Yu J., Lee S. C.: Low-temperature hydrothermal synthesis of S-doped TiO_2 with visible light photocatalytic activity. Journal of Solid State Chemistry 179 (2006) 1171-1176.
9. Liu S., Chen H.: A visible light response TiO_2 photocatalyst realized by cationic S-doping and its application for phenol degradation. Journal of Hazardous Materials 152 (2008) 48-55.

MOST WIEDZY Downloaded from mostwiedzy.pl

10. Zaleska A., Górska P., Sobczak J. W., Hupka J.: Thioacetamide and thiourea impact on visible light activity of TiO_2. Applied Catalysis B: Environmental 76 (2007) 1-8.

11. Huang D., Liao S., Quan S., Liu L., He Z., Wan J., Zhou W.: Synthesis and characterization of visible light responsive N-TiO_2 mixed crystal by a modified hydrothermal process. Journal of Non-Crystalline Solids 354 (2008) 3965-3972.

12. Asahi R., Ohikawa T., Aoki K., Taga Y.: Visible - Light Photocatalysis Nitrogen-Doped Titanium Oxides. Science 293 (2001) 269-271.

13. Górska P., Zaleska A., Kowalska E., Klimczuk T., Sobczak J. W., Skwarek E., Janusz W., Hupka J.: TiO_2 photoactivity in VIS and UV Light: The influence of calcination temperature and surface properties. Applied Catalysis B: Environmental 84 (2008) 440-447.

14. Kobayakawa K., Murakami Y., Sato Y.: Visible-light active N-doped TiO_2 prepared by heating of titanium hydroxide and urea. Journal of Photochemistry and Photobiology A: Chemistry, 170 (2005) 177-179.

15. Sakatani Y., Okusako K., Koike H., Ando H.: Proceedings of the Symposium on Recent Development of Photocatalysis. Photofunctional Materials Society of Japan (2001) 10 (abstract).

16. Yuan J., Chen M., Shi J., Shangguan W.: Preparations and photocatalytic hydrogen evolution of N-doped TiO_2 from urea and titanium tetrachloride. International Journal of Hydrogen Energy 31 (2006) 1326-1331.

17. Ao W., Li J., Yang H., Zeng X., Ma X.: Mechanochemical synthesis of zinc oxide nanocrystalline. Powder Technology 168 (2006) 148-151.

18. Bianchi C. L., Cappelletti G., Ardizzone S., Gianella S., Naldoni A., Oliva C., Pirola C.: N-doped TiO_2 from $TiCl_3$ for photodegradation of air pollutants. Catalysis Today 144 (2009) 31-36.

19. Allan N. K., Grimes C. A.: Formation of Vertically Oriented TiO2 Nanotube Arrays using a Fluoride Free HCl Aqueous Electrolyte. The Journal of Physical Chemistry C 111 (2007) 13028-13032.

20. Gunes .S., Neugebauer H., Sariciftci N. S., Roither J., Kovalenko M., Pillwein G., Heis W. Hybrid Sollar Cells Using HgTe Nanocrystals and Nanoporous TiO_2 Electrodes. Journal Material Chemistry 16 (2006) 1095-1099.

21. Bonhote P., Grätzel M., Heinen S., Walder L.: Electrochromic devices based on surface-modified nanocrystalline TiO_2 thin-film electrode. Solar Energy Materials & Solar Cells 56 (1999) 281-297.

22. Akikusa J., Kha S. U. M.: Photoresponse and IC impedance characterization of n-TiO_2 films during hydrogen and oxygen evolution reactions in an electrochemical cell. International Journal of Hydrogen Energy 22 (1997) 875-882.

23. Munoz G., Chen Q., Schmuki P.: Interfacial properties of self-organized TiO_2 nanotubes studied by impedance spectroscopy. Journal of Solid State Electrochemistry 11 (2007) 1077-1084.

MOST WIEDZY Downloaded from mostwiedzy.pl

24. Gordon F., Gomes W. P.: On the determination of the flat-band potential of a semiconductor in contact with a metal or an electrolyte from the Mott-Schottky plot. Journal of Applid Physics D 11 (1978) L63-67.

25. Madhusudan Reddy K., Baruwati B., Jaylakshmi M., Mohan Rao M., Manorama S. V.: Synthesis, characterization and redox charge transfer study, Journal of Solid State Electrochemistry 178 (2005) 3352-3358.

26. Lisowska-Oleksiak A., Szybowska K.: Polish Patent Application No P387329, Sposób otrzymywania proszku ditlenku tytanu domieszkowanego azotem.

27. Perez-Blanco J. M., Barber G. D.: Ambient atmosphere bonding of titanium foil to a transparent conductive oxide and anodic growth of titanium dioxide nanotubes. Solar Energy Materials and Solar Cells 92 (2008) 997-1002.

28. Spurr R. A., Myers H.: Quantitative Analysis of Anatase – Rutile Mixtures with an X-Ray Diffractometer. Analytical Chemistry 29 (1957) 760-762.

29. Shin H., Jung H. S., Hong K. S., Lee J. K. Crystal phase evolution of TiO_2 nanoparticles with reaction time in acidic solutions studied via freeze-drying method. Journal of Solid State Chemistry 178 (2005) 15-21.

30. Salari M., Rezaee M., Marashi S. P. H., Aboutalebi S. H.: The role of the diluent phase in the mechanochemical preparation of TiO_2 particles. Powder Technology 192 (2009) 54-57.

31. Ding J., Tsuzuki T., McCormick P .G., Street R.: Structure and magnetic properties of ultrafine Fe powders by mechanochemical processing. Journal of Magnetism and Magnetic Materials 162 (1996) 271-276.

32. Tsuzuki T., McCormick P. G.: Structure and magnetic properties of ultrafine Fe powders by mechanochemical processing. Journal of Magnetism and Magnetic Materials 162 (1996) 5143-5146.

33. Guang-Lai L., Guang-Hou W.: Morphologies of rutile from TiO_2 twin crystals. Journal of Materials Science Letters 18 (1999) 1243-1246.

34. Bai X., Xie B., Pan N., Wang X., Wang H.: Novel three-dimensional dandelion-like TiO_2 structure with high photocatalytic activity, Journal of Solid State Chemistry 181 (2008) 450-456.

35. Sakthivel S., Kisch H.: Photocatalytic and Photoelectrochemical Properties of Nitrogen-Doped Titanium Dioxide. A European Journal of Chemical Physics and Physical Chemistry 4 (2003) 487-490.

36. Zhao Y., Qiu H., Burda C.: The Effects of sintering on the Photocatalytic Activity of N-doped TiO Nanoparticles, Chemistry of Materials 20 (2008) 2629-2636.

37. Navio J. A., Cerrillos C., Real C.: Photo-inducted Transformation, upon UV Illumination in Air, of Hyponitrile Species $N_2O_2^{2-}$ Preadsorbed in TiO_2 Surface. Surface and Interface analysis 24 (1996) 355-359.

38. Li Y., Xie C., Peng S., Lu G., Li S.: Eosin Y-sensitized nitrogen-doped TiO_2 for efficient visible light photocatalytic hydrogen evolution. Journal of Molecular Catalysis A: Chemical 282 (2008) 117-123.

MOST WIEDZY Downloaded from mostwiedzy.pl

39. Liu S., Chen X., Chen X.: Preparation of N-Doped Visible-Light Response Nanosize TiO_2 Photocatalyst Using the Acid-Catalyzed Hydrolysis Method. Chinese Journal of Catalysis 27 (2006) 697-702.

40. Ihara T., Miyoshi M., Iriyama Y., Matsumoto M., Sugihara S.: Visible-light-active oxide photocatalyst realized by an oxygen-deficient structure and by nitrogen doping, Applied catalysis B: Environmental 42 (2003) 403-414.

41. NIST Standard Reference Database Number 69, http://webbook.nist.gov/chemistry/.

42. Kavan L., Grätzel M.: Highly efficient semiconducting TiO_2 photoelectrodes prepared by aerosol pyrolysis. Electrochimica Acta 40 (1995) 643-652.

43. Boukamp B. A.: Nonlinear Least Square Fit for analysis of immitance data of electrochemical systems. Solid State Ionics 20 (1986) 31-44.

44. Bard A. L., Faulkner L. R.: Electrochemical Methods: Fundamentals and Application, 2nd edn, John Wiley & Sons, Inc., New York, 2001

45. Mrowetz M., Balcerski W., Colussi A. J., Hoffmann M. R.: Oxidative power of nitrogen-doped TiO_2 photocatalysts under visible illumination. Journal of Physics Chemistry B 108 (2004) 17269-17273.

MOST WIEDZY Downloaded from mostwiedzy.pl